

Collective Quantum Entanglement in Molecular Cavity Optomechanics

Jian Huang,¹ Danyuan Lei,² Girish S. Agarwal,³ and Zhedong Zhang^{1,4,*}

¹Department of Physics, City University of Hong Kong, Kowloon, Hong Kong SAR

²Department of Materials Science and Engineering, City University of Hong Kong, Kowloon, Hong Kong SAR

³Institute for Quantum Science and Engineering, Department of Biological and Agricultural Engineering, Texas A&M University, College Station, Texas 77843, USA

⁴City University of Hong Kong, Shenzhen Research Institute, Shenzhen, Guangdong 518057, China

We propose an optomechanical scheme for reaching quantum entanglement in vibration polaritons. The system involves N molecules, whose vibrations can be fairly entangled with plasmonic cavities. We find that the vibration-photon entanglement can exist at room temperature and is robust against thermal noise. We further demonstrate the quantum entanglement between the vibrational modes through the plasmonic cavities, which shows a delocalized nature and an incredible enhancement with the number of molecules. The underlying mechanism for the entanglement is attributed to the strong vibration-cavity coupling which possesses collectivity. Our results provide a molecular optomechanical scheme which offers a promising platform for the study of noise-free quantum resources and macroscopic quantum phenomena.

Introduction.—Recent efforts have been largely devoted to studying the properties of strong coupling of molecules to light, which forms a new excitation known as the molecular polariton (MP) [1–4]. The molecular polaritons are of a wide spectrum, ranging from far infrared to ultraviolet regimes [5–8]. It has been shown an incredible modification of exciton dynamics and reaction kinetics via the strong coupling to microcavities [9–17]. Moreover, the polaritons demonstrated their quantum nature prominently in the optomechanical scheme, including Bose condensations, squeezed states, and entanglement [18, 19]. The strong molecule-photon coupling therefore led to a prosperous feature of several fields such as molecular electronics [20–22], lasers [23], and optomechanics [18, 24–26].

Molecular cavity optomechanics [27–36], known as a combination of MPs and optomechanics, is a powerful subject when exploring the spectroscopy and metrology, in which the quantum entanglement may play an important role. So far, the quantum entanglement has emerged in a variety of systems, e.g., quantum liquid [37, 38], ferromagnetic materials [39–41], and trapped ions [42]. Thanks to the advancements of cooling technique and material synthesis [43–47], cavity optomechanical model has become a promising platform to achieve prominent entanglement [48–70]. The cavity optomechanics may enable a capability of assembling entanglement robust to external noise and fluctuations. This is fairly important for an extensive study of complex materials including magnons and molecules that contain much richer degrees of freedom than atoms. Recent progresses reported the entanglement in ferromagnetic bulks against the thermal noise and disorder [40, 41]. For molecular systems, elaborate experiments demonstrated the collective coupling to cavity photons, yielding the Rabi oscillation that led to an incredibly enhanced up-conversion efficiency and a modification of matter phases [71, 72]. In this regard, the long-range coherence over many molecules arising from the collectivity turns out to be of a central aspect, so as to combat the local fluctuations. This however is still an open issue.

The collective molecule-cavity interaction essentially

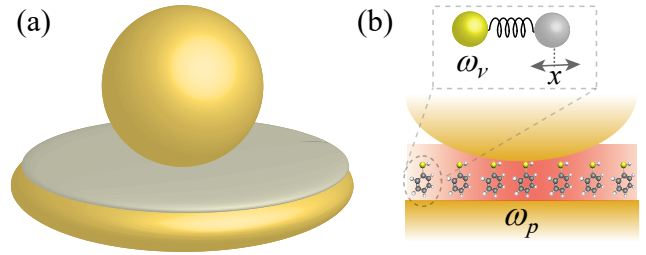


FIG. 1. (a) Schematic of the nanoparticle-on-mirror configuration. From top to bottom, they are metallic nanoparticle, self-assembled monolayer of thiophenol molecules, and metallic substrate, respectively. (b) Schematic of the molecular cavity optomechanical system. Plasmonic cavity mode (with resonance frequency ω_p) is coupled to N molecular vibrational modes (resonance frequency ω_v) via the optomechanical interactions. Here the vibrational mode is depicted as two masses linked by a spring.

brings out a \sqrt{N} enhancement of the optomechanical coupling [73, 74]. This used to be a hard task in the cavity optomechanics. In this Letter, we study the quantum entanglement in the molecular cavity optomechanical systems. The \sqrt{N} scaling is shown to be a key for reaching the entanglement between molecular vibrations. We find that, under feasible parameter regimes, the cavity-vibration entanglement can survive at room temperature and is highly robust to the thermal noise. Moreover, our results reveal a delocalized nature of the vibration-vibration entanglement, evident by the unusual scaling of the logarithmic negativity against the size of molecular sample. This further leads to a remarkable enhancement when having a large number of molecules in the sample. Our work offers a new paradigm for generating quantum resources and for studying the quantum information processing using molecular optomechanical systems.

Molecular model and Langevin equations.—We consider a molecular cavity optomechanical system consisting of a plasmonic cavity and N identical molecules. The plasmonic system can be realized in the nanoparticle-on-mirror configuration [75] or the scanning-tunnelling microscope tip on

metallic substrate [76], where N organic molecules are sandwiched in the gap between the nanostructure and the metallic substrate (see Fig. 1). Molecular optomechanics possesses two notable advantages: (i) high molecule-photon coupling from the tightly-confined mode volume of cavities; (ii) high vibration frequency where the thermalization is suppressed at room temperature, that is significant for quantum applications. In this vein, the molecular optomechanical system provide a promising platform for investigating quantum entanglement. In the low-excitation-number case, the vibrational mode of each molecule can be approximately described by a harmonic oscillator with resonance frequency ω_v and a normal coordinate $x = x_{zpf}(b^\dagger + b)$, where x_{zpf} is the zero-point amplitude and b (b^\dagger) is the annihilation (creation) operator. We assume that the cavity resonance frequency ω_p is off-resonant with the optically allowed electronic transitions of the molecule. The vibration-cavity coupling is thus parametric. The molecular vibration thus modulates the cavity resonance frequency, i.e., $\omega_p(x) \approx \omega_p - \tilde{g}_v x$, where $\tilde{g}_v = \omega_p(\partial\alpha/\partial x)/(\epsilon_0 V_p)$, with α , ϵ_0 , and V_p being the respective polarizability of the molecule, the vacuum permittivity, and the volume of the cavity [27]. The Hamiltonian of the system is of the form ($\hbar = 1$)

$$H = \omega_p a^\dagger a + \sum_{j=1}^N [\omega_v b_j^\dagger b_j + g_v a^\dagger a (b_j^\dagger + b_j)] + (\Omega a^\dagger e^{-i\omega t} + \text{H.c.}), \quad (1)$$

where a (a^\dagger) and b_j (b_j^\dagger) are the annihilation (creation) operators of the cavity mode and the vibrational mode of the j th molecule, respectively. $g_v = -\tilde{g}_v x_{zpf}$ is the molecular optomechanical coupling constant [77]; Ω and ω_l are the amplitude and frequency of the pump field, respectively. With the effective mass of the vibrations, one finds $g_v = -\omega_p R_v \sqrt{\hbar/2m\omega_v}/(\epsilon_0 V_p)$, where $R_v = \partial\alpha/\partial x$ and α is the Raman polarizability. As an estimation [27], $\omega_p/2\pi = 333$ THz, $\omega_v/2\pi = 29.9$ THz, $R_v^2/m \approx 3 \times 10^{-10} \epsilon_0^2 \text{\AA}^4 \text{amu}^{-1}$, and $V_p = 1.5 \times 10^{-6} \mu\text{m}^3$, which yield $-g_v/2\pi \approx 21$ GHz. In recent studies, for both theory [27, 28, 34] and experiments [29, 31, 76], the parameters were taken as $-g_v/2\pi \sim 10$ GHz-100 GHz and $\omega_v/2\pi \sim 6$ THz-48 THz ($\approx 200 \text{ cm}^{-1}$ -1600 cm^{-1}).

We consider a large number of molecules in the cavity, i.e., $N \gg 1$, that is always feasible in labs. Our motivation is to study the entanglement between the molecules. To this end, one defines the two collective vibrational modes $B_1 = \sum_{j=1}^M b_j/\sqrt{M}$ and $B_2 = \sum_{j=M+1}^N b_j/\sqrt{N-M}$ (with $[B_l, B_l^\dagger] = \delta_{ll}$) [78, 79]. The Hamiltonian H in the rotating frame of the drive frequency ω_l can be rewritten as

$$H_l = \Delta_p a^\dagger a + \sum_{l=1}^2 [\omega_v B_l^\dagger B_l + g_l a^\dagger a (B_l^\dagger + B_l)] + (\Omega a^\dagger + \text{H.c.}), \quad (2)$$

where $\Delta_p = \omega_p - \omega_l$ is the driving detuning, and $g_1 = g_v \sqrt{M}$ ($g_2 = g_v \sqrt{N-M}$) is the collective optomechanical coupling strength between the cavity mode a and the collective vibrational mode B_1 (B_2).

With a strong drive, the dynamics of this system can be linearized by writing each operator into $o = \langle o \rangle_{ss} + \delta o$, where $\langle o \rangle_{ss}$ and δo denote the steady-state mean and the quantum fluctuation, respectively. The linearized quantum Langevin equations are thus obtained

$$\begin{aligned} \delta \dot{a} &= -(i\Delta + \kappa)\delta a - i \sum_{l=1}^2 G_l (\delta B_l^\dagger + \delta B_l) + \sqrt{2\kappa} a_{in}, \\ \delta \dot{B}_1 &= -(i\omega_v + \gamma_1)\delta B_1 - i(G_1^* \delta a + G_1 \delta a^\dagger) + \sqrt{2\gamma} B_{1,in}, \\ \delta \dot{B}_2 &= -(i\omega_v + \gamma_2)\delta B_2 - i(G_2^* \delta a + G_2 \delta a^\dagger) + \sqrt{2\gamma} B_{2,in}, \end{aligned} \quad (3)$$

where κ and $\gamma_{l=1,2}$ are the decay rates of the cavity mode and collective vibrational modes, respectively; $\Delta = \Delta_p + \sum_{l=1}^2 g_l (\langle B_l \rangle_{ss} + \langle B_l \rangle_{ss}^*)$ is the normalized driving detuning; $G_1 = \sqrt{M} G_v$ and $G_2 = \sqrt{N-M} G_v$ ($G_v = g_v \langle a \rangle_{ss}$) are the linearized collective (single-photon) optomechanical coupling strengths. The collectivity of G_l in the molecular cavity optomechanics may lead to the ultrastrong-coupling regime, while it used to be weak in conventional optomechanics. Thus the term $G_l \delta B_l^\dagger$ in Eq. (3) resulting from the counter-rotating-wave effect cannot be neglected, and it is the key component for generating entanglement. Elaborate analysis will be presented later on. The steady-state means are

$$\langle a \rangle_{ss} = \frac{-i\Omega}{i\Delta + \kappa}, \quad \langle B_l \rangle_{ss} = \frac{-ig_l \langle a \rangle_{ss}}{i\omega_v + \gamma_l}. \quad (4)$$

The noise operators a_{in} , $B_{1,in} = \sum_{j=1}^M b_{j,in}/\sqrt{M}$, and $B_{2,in} = \sum_{j=M+1}^N b_{j,in}/\sqrt{N-M}$ are characterized by the nonzero correlation functions [80], $\langle a_{in}(t) a_{in}^\dagger(t') \rangle = \delta(t-t')$, $\langle B_{l,in}(t) B_{l,in}^\dagger(t') \rangle = (\bar{n}_l + 1)\delta(t-t')$, and $\langle B_{l,in}^\dagger(t) B_{l,in}(t') \rangle = \bar{n}_l \delta(t-t')$, with \bar{n}_l being the thermal phonon number for the vibrational mode B_l .

By defining the vectors of the quadrature fluctuation operators $\mathbf{u}(t) = (\delta X_{B_1}, \delta Y_{B_1}, \delta X_{B_2}, \delta Y_{B_2}, \delta X_a, \delta Y_a)^T$ and the noise operators $\mathbf{N}(t) = \sqrt{2}(\sqrt{\gamma_1} X_{B_1}^{in}, \sqrt{\gamma_1} Y_{B_1}^{in}, \sqrt{\gamma_2} X_{B_2}^{in}, \sqrt{\gamma_2} Y_{B_2}^{in}, \sqrt{\kappa} X_a^{in}, \sqrt{\kappa} Y_a^{in})^T$, with $\delta X_o = (\delta o^\dagger + \delta o)/\sqrt{2}$, $\delta Y_o = i(\delta o^\dagger - \delta o)/\sqrt{2}$, $X_o^{in} = (o_{in}^\dagger + o_{in})/\sqrt{2}$, and $Y_o^{in} = i(o_{in}^\dagger - o_{in})/\sqrt{2}$ for $o_{in} = a_{in}$ and $B_{l,in}$, the Eqs. (3) can be expressed concisely as $\dot{\mathbf{u}}(t) = \mathbf{A}\mathbf{u}(t) + \mathbf{N}(t)$, where the drift matrix \mathbf{A} is given by

$$\mathbf{A} = \begin{pmatrix} -\gamma_1 & \omega_v & 0 & 0 & 0 & 0 \\ -\omega_v & -\gamma_1 & 0 & 0 & -2G_1^{\text{Re}} & -2G_1^{\text{Im}} \\ 0 & 0 & -\gamma_2 & \omega_v & 0 & 0 \\ 0 & 0 & -\omega_v & -\gamma_2 & -2G_2^{\text{Re}} & -2G_2^{\text{Im}} \\ 2G_1^{\text{Im}} & 0 & 2G_2^{\text{Im}} & 0 & -\kappa & \Delta \\ -2G_1^{\text{Re}} & 0 & -2G_2^{\text{Re}} & 0 & -\Delta & -\kappa \end{pmatrix}. \quad (5)$$

Here $G_{l=1,2}^{\text{Re}}$ (G_l^{Im}) is the real (imaginary) part of G_l . This linearized system can achieve stability only if the real parts of the eigenvalues of \mathbf{A} are negative, as delineated by the Routh-Hurwitz criterion [81].

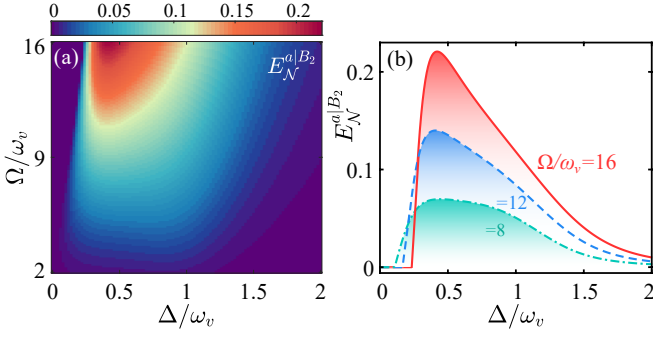


FIG. 2. Logarithmic negativity (a) $E_N^{a|B_2}$ versus the detuning Δ/ω_v and the driving amplitude Ω/ω_v . (b) $E_N^{a|B_2}$ versus Δ/ω_v for different values of Ω . Other parameters used are $\gamma_{l=1,2}/\omega_v = 10^{-4}$, $\kappa/\omega_v = 1/3$, $M = 0$, $N = 100$, and $\bar{n} = 0.01$.

To explore the steady-state quantum entanglement, we introduce the covariance matrix \mathbf{V} , which is characterized by the matrix elements as $\mathbf{V}_{ij} = \frac{1}{2}[\langle \mathbf{u}_i(\infty) \mathbf{u}_j(\infty) \rangle + \langle \mathbf{u}_j(\infty) \mathbf{u}_i(\infty) \rangle]$ for $i, j = 1-6$. The covariance matrix \mathbf{V} is determined by the Lyapunov equation $\mathbf{A}\mathbf{V} + \mathbf{V}\mathbf{A}^T = -\mathbf{Q}$ [50], where $\mathbf{Q} = \text{diag}\{(2\bar{n}_1 + 1)\gamma_1, (2\bar{n}_1 + 1)\gamma_1, (2\bar{n}_2 + 1)\gamma_2, (2\bar{n}_2 + 1)\gamma_2, \kappa, \kappa\}$ represents the diffusion matrix.

Generating cavity-vibration entanglement.—To measure quantum entanglement of the system, we initially provide the definition of logarithmic negativity. For a two-mode system composed by bosonic modes C and D , its covariance matrix \mathcal{V} can be represented as $\mathcal{V} = \{\{\mathcal{V}_C, \mathcal{V}_{CD}\}, \{\mathcal{V}_{CD}^T, \mathcal{V}_D\}\}$, where \mathcal{V}_C , \mathcal{V}_{CD} , and \mathcal{V}_D are, respectively, the block matrices associated with the mode C , the correlation term, and the mode D . The definition of logarithmic negativity [82–84] is

$$E_N = \max[0, -\ln(2\eta^-)], \quad (6)$$

where $\eta^- = 2^{-1/2}[\Sigma(\mathcal{V}) - [\Sigma(\mathcal{V})^2 - 4\det\mathcal{V}]^{1/2}]^{1/2}$ is the minimum symplectic eigenvalue of the matrix \mathcal{V} , with $\Sigma(\mathcal{V}) = \det\mathcal{V}_C + \det\mathcal{V}_D - 2\det\mathcal{V}_{CD}$. For our system, the quantum entanglement between the two modes a and B_l (B_1 and B_2) is represented by the logarithmic negativity $E_N^{a|B_l}$ ($E_N^{B_l|B_2}$). The reduced matrix \mathcal{V} of two involved modes is obtained by tracing out the uncorrelated rows and columns in the covariance matrix \mathbf{V} .

Since the two types cavity-vibration entanglement ($E_N^{a|B_1}$ and $E_N^{a|B_2}$) exhibit similar behaviors with the change of the adjustable parameters, in Fig. 2 we only show $E_N^{a|B_2}$ versus the detuning Δ and the driving amplitude Ω . In the numerical simulations, we adopt parameters that are experimentally achievable: $\omega_l/2\pi = 300$ THz, $\omega_v/2\pi = 30$ THz, $\kappa/2\pi = 10$ THz, $\gamma_1/2\pi = \gamma_2/2\pi = 0.03$ THz, $g_v/2\pi = 30$ GHz, $T \approx 312$ K, $M = 0$, and $N = 100$. For the vibrational-mode frequency $\omega_v/2\pi = 30$ THz, the corresponding thermal phonon number of vibrational mode can be estimated as $\bar{n}_l = \bar{n} = 0.01$ when $T \approx 312$ K. For convenience, we take the vibrational-mode frequency ω_v as the scaling unit in the following numerical simulations. Figure 2 shows that $E_N^{a|B_2}$

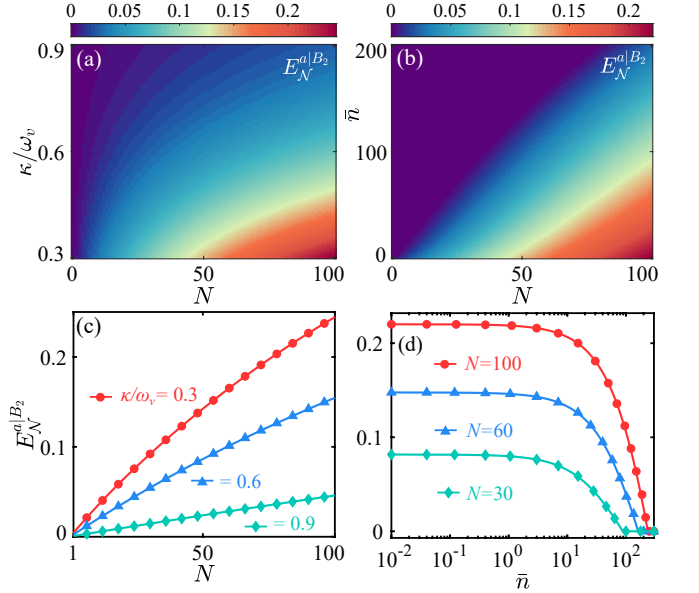


FIG. 3. $E_N^{a|B_2}$ versus the number of molecules N and the decay rate κ/ω_v . (b) $E_N^{a|B_2}$ versus N and the thermal phonon excitation number \bar{n} . $E_N^{a|B_2}$ versus (c) N and (d) \bar{n} . Here $\Delta/\omega_v = 0.4$, $\Omega/\omega_v = 16$, and other parameters are the same as those in Fig. 2.

reaches a peak value around the optimal detuning $\Delta/\omega_v \approx 0.4$ when Ω takes maximum value. However, the cavity mode and the vibrational mode are uncorrelated when Ω has a small value. The reason is that the existence of entanglement requires a large effective coupling strength $G_2 = \sqrt{N}g_v\langle a \rangle_{ss}$, i.e., a strong pump field with a large amplitude Ω . Notice that we study the entanglement in the red-detuned regime, because of a large coupling strength ($|G_2|/\omega_v \approx 0.31$ when $\Omega/\omega_v = 16$ and $\Delta/\omega_v = 0.4$) that may generate considerable entanglement [50, 53]. This falls into the ultrastrong coupling regime in which the counter-rotating-wave term $G_2(\delta a \delta B_2 + \delta a^\dagger \delta B_2^\dagger)$ survives. It turns out to be crucial for creating the entanglement [85].

To investigate the dependence of cavity-vibration entanglement on the collective coupling strength ($\sqrt{N}G_v$), in Fig. 3(a) and 3(c) we depict the $E_N^{a|B_2}$ versus the number of molecules N and the decay rate κ . The results show that $E_N^{a|B_2}$ increases with the number N , and the maximum value of $E_N^{a|B_2}$ can reach is smaller for the higher decay rates. The underlying physics for this phenomenon is that $E_N^{a|B_2}$ is a monotonically increasing function of the collective coupling strength $G_2 = \sqrt{N}G_v$. The increase in number N can greatly enhance the G_2 , thereby correspondingly enhancing the cavity-vibration entanglement. However, the decay rate κ of cavity mode is a detrimental factor in the creation of entanglement. In Fig. 3(b), we show the robust quantum entanglement against the thermal noise by plotting the $E_N^{a|B_2}$ as function of number N and the thermal phonon excitation number \bar{n} . The curves in Fig. 3(d) show that $E_N^{a|B_2}$ can still exist even when the thermal phonon numbers in the vibrational mode are about $\bar{n} = 200$, which implies

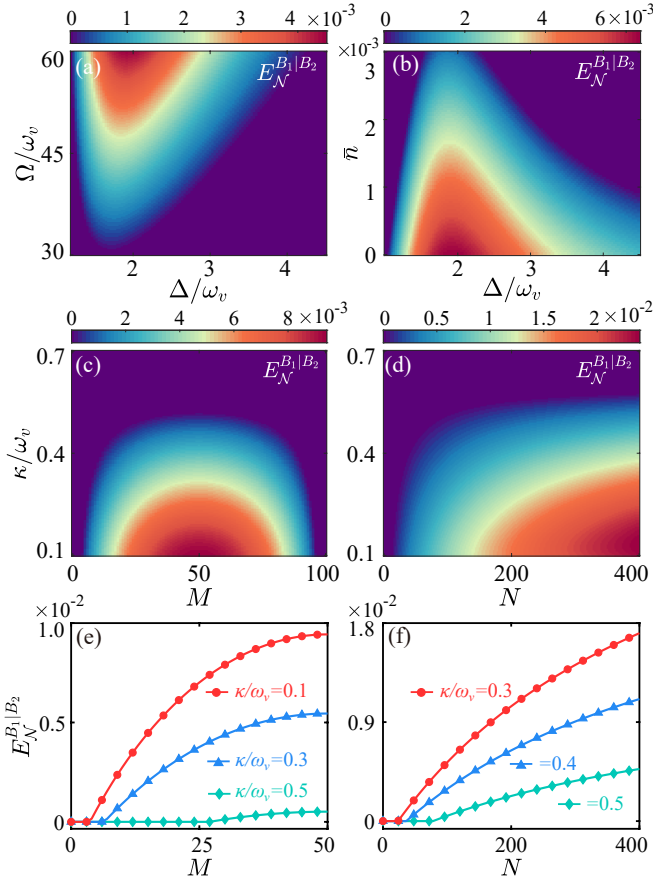


FIG. 4. (a) $E_N^{B_1|B_2}$ versus the scaled detuning Δ/ω_v and Ω/ω_v . (b) $E_N^{B_1|B_2}$ versus Δ/ω_v , and thermal phonon numbers \bar{n} . (c) $E_N^{B_1|B_2}$ versus M and the scaled decay rate κ/ω_v . (d) $E_N^{B_1|B_2}$ versus the total number of molecules N and κ/ω_v when $M = N/2$. $E_N^{B_1|B_2}$ versus (e) M and (f) N for different values of κ . Here $\Omega/\omega_v = 60$, $\gamma_l/\omega_v = 0.3$, $\Delta/\omega_v = 2$, $M = 50$, and $\bar{n}_1 = \bar{n}_2 = 0.001$ ($T \approx 210$ K) when they are not variables, and other parameters are the same as those in Fig 2.

that the cavity-vibration entanglement can not only emerge in environments far above room temperature ($T \approx 312$ K), but also possesses strong robustness against thermal noise.

Generating vibration-vibration entanglement.—Since the investigated system involves two collective vibrational modes coupled to the plasmonic cavity, a natural question emerges: can the plasmonic cavity induce quantum entanglement between the two collective vibrational modes? To clarify this issue, it is essential to derive a reduced Hamiltonian containing only two collective vibrational modes. In the large cavity-decay regime, by adiabatically eliminating the cavity mode [77], the effective Hamiltonian can be expressed as

$$H_{\text{eff}} \approx \sum_{l=1}^2 (\Omega_l - i\Gamma_l) \delta B_l^\dagger \delta B_l - i\mathcal{G} (\delta B_1^\dagger - \delta B_1) (\delta B_2^\dagger - \delta B_2), \quad (7)$$

where Ω_l and Γ_l are the effective frequency and decay rate of the l th collective vibration mode, respectively; $\mathcal{G} \approx (i/2\omega_v - 1/\kappa)G_1G_2$ is the effective coupling strength [77].

In Fig. 4(a) we study the vibration-vibration entanglement by plotting $E_N^{B_1|B_2}$ as function of Δ and Ω . The results show that the optimal detuning for the peak value of $E_N^{B_1|B_2}$ is located around $\Delta/\omega_v \approx 2$, and a considerable driving amplitude Ω is required to generate vibration-vibration entanglement. This phenomenon can be explained by: As the detuning Δ increases, a stronger driving amplitude is necessary to yield a larger effective coupling ($|G_{l=1,2}|/\omega_v \approx 0.21$ when $\Omega/\omega_v = 60$ and $\Delta/\omega_v = 2$). We also find that the vibration-vibration entanglement is much smaller than cavity-vibration entanglement, because there is no direct interaction between the two collective vibrational modes, and the indirect coupling $i\mathcal{G}$ induced by cavity mode is much smaller than G_1 and G_2 . Moreover, the vibration-vibration entanglement is exceedingly susceptible to thermal noise ($E_N^{B_1|B_2} = 0$ when $\bar{n} > 0.003$), as shown in Fig. 4(b).

To further investigate the dependence of vibration-vibration entanglement on the number of molecules, in Figs. 4(c) and 4(e) we plot $E_N^{B_1|B_2}$ versus the number M (in the collective mode B_1) and decay rate κ . The results show that $E_N^{B_1|B_2}$ initially start at zero, as the number M increases, $E_N^{B_1|B_2}$ correspondingly rises, reaching a peak value at the point $M = 50$. Following this, $E_N^{B_1|B_2}$ decreases back to zero in the remaining region. This phenomenon can be elucidated by the indirect coupling strength \mathcal{G} , which is determined by the product of two collective optomechanical coupling strengths ($\mathcal{G} \propto \sqrt{MG_v} \times \sqrt{N-MG_v}$). In this scenario, the induced coupling strength reaches its maximum when $M = 50$, resulting in the strongest vibration-vibration entanglement. On the contrary, the entanglement becomes relatively weak and may even be completely disrupted by thermal noise when M takes a larger or smaller value.

In Figs. 4(d) and 4(f), we study the influence of total number of molecules N on the vibration-vibration entanglement. Figure 4(d) shows that $E_N^{B_1|B_2}$ grows from initial 0 to a larger value 0.018 with the number N increases. Because the increase of the number N can significantly enhance the indirect coupling between the two collective modes, transforming them from independent to strongly entangled. Moreover, we observed from Fig 4(f) that $E_N^{B_1|B_2}$ exhibits a approximate linear growth with respect to the total number N , the reason may be that the induced indirect coupling strength \mathcal{G} is proportional to N ($\propto NG_v^2/2$) when we set the parameter condition $M = N/2$.

Finally, the quantum entanglement can be measured by the time-resolved detection of photons emitted from the plasmonic cavity field. Concretely, the cavity mode quadratures can be measured by homodyne detection of the cavity output. The vibrational mode quadratures can be transferred to time-gated emitted photons, which can then be homodyne detected through interference using an additional microwave field. The cavity homodyned signal and the molecular homodyned signal can be used to find the correlations involving field and vibration quadratures.

Conclusion.—Our scheme of molecular optomechanics

works with the red detuning. This is distinct from the blue-detuning of which the cavity magnomechanics is in favor but the molecular optomechanics may not [40, 41]. Here the blue detuning yields a narrow window for the optomechanical coupling, i.e., $G_i \lesssim 0.006\omega_v$ due to the stability [50]. Nevertheless, the red detuning leads to $G_i \lesssim 0.6\omega_v$ which is much broader. Therefore the molecular optomechanical systems are in favor of the red detuning rather than the blue one, for creating strong entanglement. Our calculations reveal an entanglement $\lesssim 7 \times 10^{-4}$ in the blue-detuned regime.

In summary, we developed a molecular cavity optomechanical scheme for generating the quantum entanglement in the collective vibrations of molecular ensembles. The results highlighted the role of the significant collective enhancement (i.e., \sqrt{N} scaling) which yields a strong molecule-cavity entanglement at room temperature with experimentally feasible parameters. The results further revealed the quantum entanglement between the vibrational modes which shows a long-range nature and a dramatic enhancement with the number of molecules. Our scheme offers a new paradigm for the quantum interfaces between molecules and plasmonic cavities. These may form promising platforms of quantum information processing and reactivity control, where the molecular vibrations can function as the information storage medium that can be transferred to others.

We thank Deng-Gao Lai, Ya-Feng Jiao, and Jing-Xue Liu for helpful discussions. Z.Z. and J.H. gratefully acknowledge the support of the Early Career Scheme from Hong Kong Research Grants Council (No. 21302721), the National Science Foundation of China (No. 12104380), and the National Science Foundation of China/RGC Collaborative Research Scheme (No. CRS-CUHK401/22). D. L. gratefully acknowledges the support of the National Science Foundation of China, the Excellent Young Scientist Fund (No. 62022001). G.S.A thanks the Air Force Office of Scientific Research (Award No. FA-9550-20-1-0366) and the Robert A. Welch Foundation (Grant No. A-1943-20210327).

* zzhan26@cityu.edu.hk

- [1] S. Aberra Guebrou, C. Symonds, E. Homeyer, J. C. Plenet, Yu. N. Gartstein, V. M. Agranovich, and J. Bellessa, Coherent Emission from a Disordered Organic Semiconductor Induced by Strong Coupling with Surface Plasmons, *Phys. Rev. Lett.* **108**, 066401 (2012).
- [2] F. C. Spano, Optical microcavities enhance the exciton coherence length and eliminate vibronic coupling in J-aggregates, *J. Chem. Phys.* **142**, 184707 (2015).
- [3] J. Flick, M. Ruggenthaler, H. Appel, and A. Rubio, Atoms and molecules in cavities, from weak to strong coupling in quantum-electrodynamics (QED) chemistry, *Proc. Natl. Acad. Sci. U.S.A.* **114**, 3026 (2017)
- [4] R. Su, S. Ghosh, J. Wang, S. Liu, C. Diederichs, T. C. H. Liew, and Q. Xiong, Observation of exciton polariton condensation in a perovskite lattice at room temperature, *Nat. Phys.* **16**, 301 (2020).
- [5] B. Xiang, R. F. Ribeiro, A. D. Dunkelberger, J. Wang, Y. Li, B. S. Simpkins, J. C. Owrutsky, J. Yuen-Zhou, and W. Xiong, Two-dimensional infrared spectroscopy of vibrational polaritons, *Proc. Natl. Acad. Sci. U.S.A.* **115**, 4845 (2018).
- [6] R. F. Ribeiro, A. D. Dunkelberger, B. Xiang, W. Xiong, B. S. Simpkins, J. C. Owrutsky, and J. Yuen-Zhou, Theory for Nonlinear Spectroscopy of Vibrational Polaritons, *J. Phys. Chem. Lett.* **9**, 3766 (2018).
- [7] Z. D. Zhang, K. Wang, Z. Yi, M. S. Zubairy, M. O. Scully, and S. Mukamel, Polariton-assisted cooperativity of molecules in microcavities monitored by two-dimensional infrared spectroscopy, *J. Phys. Chem. Lett.* **10**, 4448 (2019).
- [8] Z. Zhang, X. Nie, D. Lei, and S. Mukamel, Multidimensional Coherent Spectroscopy of Molecular Polaritons: Langevin Approach, *Phys. Rev. Lett.* **130**, 103001 (2023).
- [9] J. Hutchison, T. Schwartz, C. Genet, E. Devaux, and T. W. Ebbesen, Modifying chemical landscapes by coupling to vacuum fields, *Angew. Chem.* **124**, 1624 (2012).
- [10] D. M. Coles, N. Somaschi, P. Michetti, C. Clark, P. G. Lagoudakis, P. G. Savvidis, and D. G. Lidzey, Polariton-mediated energy transfer between organic dyes in a strongly coupled optical microcavity, *Nat. Mater.* **13**, 712 (2014).
- [11] A. Thomas, J. George, A. Shalabney, M. Dryzhakov, S. J. Varma et al., Ground-state chemical reactivity under vibrational coupling to the vacuum electromagnetic field, *Angew. Chem., Int. Ed.* **55**, 11462 (2016).
- [12] A. D. Dunkelberger, B. T. Spann, K. P. Fears, B. S. Simpkins, and J. C. Owrutsky, Modified relaxation dynamics and coherent energy exchange in coupled vibration-cavity polaritons, *Nat. Commun.* **7**, 13504 (2016).
- [13] F. Herrera and F. C. Spano, Cavity-Controlled Chemistry in Molecular Ensembles, *Phys. Rev. Lett.* **116**, 238301 (2016).
- [14] M. Kowalewski, K. Bennett, and S. Mukamel, Cavity femtochemistry: Manipulating nonadiabatic dynamics at avoided crossings, *J. Phys. Chem. Lett.* **7**, 2050 (2016).
- [15] J. Galego, F. J. Garcia-Vidal, and J. Feist, Suppressing photochemical reactions with quantized light fields, *Nat. Commun.* **7**, 13841 (2016).
- [16] L. Martinez-Martinez, R. Ribeiro, J. Campos-Gonzalez-Angulo, and J. Yuen-Zhou, Can ultrastrong coupling change ground-state chemical reactions? *ACS Photonics* **5**, 167 (2018).
- [17] X. Li, A. Mandal, and P. Huo, Cavity frequency-dependent theory for vibrational polariton chemistry, *Nat. Commun.* **12**, 1315 (2021).
- [18] M. Aspelmeyer, T. J. Kippenberg, and F. Marquardt, Cavity optomechanics, *Rev. Mod. Phys.* **86**, 1391 (2014).
- [19] M. Metcalfe, Applications of cavity optomechanics, *Appl. Phys. Rev.* **1**, 031105 (2014).
- [20] C. Joachim, J. K. Gimzewski, and A. Aviram, Electronics using hybrid-molecular and mono-molecular devices, *Nature (London)* **408**, 541 (2000).
- [21] J. C. Cuevas and E. Scheer, *Molecular Electronics: An Introduction to Theory and Experiment* (World Scientific, Singapore, 2010).
- [22] D. Xiang, X. L. Wang, C. C. Jia, T. Lee, and X. F. Guo, Molecular-scale electronics: from concept to function, *Chem. Rev.* **116**, 4318 (2016).
- [23] S. Kena-Cohen and S. R. Forrest, Room-temperature polariton lasing in an organic single-crystal microcavity, *Nat. Photonics* **4**, 371 (2010).
- [24] A. Shalabney, J. George, J. A. Hutchison, G. Pupillo, C. Genet, and T. W. Ebbesen, Coherent coupling of molecular resonators with a microcavity mode, *Nat. Commun.* **6**, 5981 (2015).
- [25] J. Pino, J. Feist, and F. J. Garcia-Vidal, Quantum theory

- of collective strong coupling of molecular vibrations with a microcavity mode, *New J. Phys.* **17**, 053040 (2015).
- [26] B. Xiang and W. Xiong, Molecular polaritons for chemistry, photonics and quantum Technologies, *Chem. Rev.* **124**, 2512 (2024)
- [27] P. Roelli, C. Galland, N. Piro, and T. J. Kippenberg, Molecular cavity optomechanics as a theory of plasmon-enhanced Raman scattering, *Nat. Nanotechnol.* **11**, 164 (2016).
- [28] M. K. Schmidt, R. Esteban, A. Gonzalez-Tudela, G. Giedke, and J. Aizpurua, Quantum mechanical description of Raman scattering from molecules in plasmonic cavities, *ACS Nano.* **10**, 6291 (2016).
- [29] F. Benz *et al.*, Single-molecule optomechanics in “picocavities”, *Science* **354**, 726 (2016).
- [30] M. K. Dezfouli and S. Hughes, Quantum optics model of surface-enhanced Raman spectroscopy for arbitrarily shaped plasmonic resonators, *ACS Photonics* **4**, 1245 (2017).
- [31] A. Lombardi, M. K. Schmidt, L. Weller, W. M. Deacon, F. Benz, B. de Nijs, J. Aizpurua, and J. J. Baumberg, Pulsed Molecular Optomechanics in Plasmonic Nanocavities: From Nonlinear Vibrational Instabilities to Bond-Breaking, *Phys. Rev. X* **8**, 011016 (2018).
- [32] T. Neuman, R. Esteban, G. Giedke, M. K. Schmidt, and J. Aizpurua, Quantum description of surface-enhanced resonant Raman scattering within a hybrid-optomechanical model, *Phys. Rev. A* **100**, 043422 (2019).
- [33] Y. Zhang, J. Aizpurua, and R. Esteban, Optomechanical collective effects in surface-enhanced Raman scattering from many molecules, *ACS Photonics* **7**, 1676 (2020)
- [34] R. Esteban, J. J. Baumberg, and J. Aizpurua, Molecular optomechanics approach to surface-enhanced Raman scattering, *Acc. Chem. Res.* **55**, 1889 (2022).
- [35] L. A. Jakob, *et al.*, Giant optomechanical spring effect in plasmonic nano- and picocavities probed by surface-enhanced Raman scattering, *Nat. Commun.* **14**, 3291 (2023).
- [36] A. Koner, M. Du, S. Pannir-Sivajothi, R. H. Goldsmith, and J. Yuen-Zhou, A path towards single molecule vibrational strong coupling in a Fabry-Perot microcavity, *Chem. Sci.* **14**, 7753 (2023)
- [37] Y. Zhou, K. Kanoda, and T.-K. Ng, Quantum spin liquid states, *Rev. Mod. Phys.* **89**, 025003 (2017).
- [38] L. Savary and L. Balents, Quantum spin liquids: a review, *Rep. Prog. Phys.* **80**, 016502 (2017).
- [39] S. Ghosh, T. F. Rosenbaum, G. Aeppli, and S. N. Coppersmith, Entangled quantum state of magnetic dipoles, *Nature (London)* **425**, 48 (2003).
- [40] J. Li, S.-Y. Zhu, and G. S. Agarwal, Magnon-Photon-Phonon Entanglement in Cavity Magnomechanics, *Phys. Rev. Lett.* **121**, 203601 (2018).
- [41] Z. Zhang, M. O. Scully, and G. S. Agarwal, Quantum entanglement between two magnon modes via Kerr nonlinearity driven far from equilibrium, *Phys. Rev. Research* **1**, 023021 (2019).
- [42] D. Leibfried, R. Blatt, C. Monroe, and D. Wineland, Quantum dynamics of single trapped ions, *Rev. Mod. Phys.* **75**, 281 (2003).
- [43] I. Wilson-Rae, N. Nooshi, W. Zwerger, and T. J. Kippenberg, Theory of Ground State Cooling of a Mechanical Oscillator Using Dynamical Backaction, *Phys. Rev. Lett.* **99**, 093901 (2007).
- [44] F. Marquardt, J. P. Chen, A. A. Clerk, and S. M. Girvin, Quantum Theory of Cavity-Assisted Sideband Cooling of Mechanical Motion, *Phys. Rev. Lett.* **99**, 093902 (2007).
- [45] J. Chan, T. P. Alegre, A. H. Safavi-Naeini, J. T. Hill, A. Krause, S. Groblacher, M. Aspelmeyer, and O. Painter, Laser cooling of a nanomechanical oscillator into its quantum ground state, *Nature (London)* **478**, 89 (2011).
- [46] J. D. Teufel, T. Donner, D. Li, J. W. Harlow, M. S. Allman, K. Cicak, A. J. Sirois, J. D. Whittaker, K. W. Lehnert, and R. W. Simmonds, Sideband cooling of micromechanical motion to the quantum ground state, *Nature (London)* **475**, 359 (2011).
- [47] S. Barzanjeh, A. Xuereb, S. Gröblacher, M. Paternostro, C. A. Regal, and E. M. Weig, Optomechanics for quantum technologies, *Nat. Phys.* **18**, 15 (2022).
- [48] S. Mancini, V. Giovannetti, D. Vitali, and P. Tombesi, Entangling Macroscopic Oscillators Exploiting Radiation Pressure, *Phys. Rev. Lett.* **88**, 120401 (2002).
- [49] S. Pirandola, D. Vitali, P. Tombesi, and S. Lloyd, Macroscopic Entanglement by Entanglement Swapping, *Phys. Rev. Lett.* **97**, 150403 (2006).
- [50] D. Vitali, S. Gigan, A. Ferreira, H. R. Böhm, P. Tombesi, A. Guerreiro, V. Vedral, A. Zeilinger, and M. Aspelmeyer, Optomechanical Entanglement between a Movable Mirror and a Cavity Field, *Phys. Rev. Lett.* **98**, 030405 (2007).
- [51] D. Vitali, S. Mancini, and P. Tombesi, Stationary entanglement between two movable mirrors in a classically driven Fabry-Perot cavity, *J. Phys. A: Math. Theor.* **40**, 8055 (2007).
- [52] M. Paternostro, D. Vitali, S. Gigan, M. S. Kim, C. Brukner, J. Eisert, and M. Aspelmeyer, Creating and Probing Multipartite Macroscopic Entanglement with Light, *Phys. Rev. Lett.* **99**, 250401 (2007).
- [53] C. Genes, A. Mari, P. Tombesi, and D. Vitali, Robust entanglement of a micromechanical resonator with output optical fields, *Phys. Rev. A* **78**, 032316 (2008).
- [54] M. J. Hartmann and M. B. Plenio, Steady State Entanglement in the Mechanical Vibrations of Two Dielectric Membranes, *Phys. Rev. Lett.* **101**, 200503 (2008).
- [55] K. Børkje, A. Nunnenkamp, and S. M. Girvin, Proposal for Entangling Remote Micromechanical Oscillators via Optical Measurements, *Phys. Rev. Lett.* **107**, 123601 (2011).
- [56] M. Abdi, S. Pirandola, P. Tombesi, and D. Vitali, Entanglement Swapping with Local Certification: Application to Remote Micromechanical Resonators, *Phys. Rev. Lett.* **109**, 143601 (2012).
- [57] L. Tian, Robust Photon Entanglement via Quantum Interference in Optomechanical Interfaces, *Phys. Rev. Lett.* **110**, 233602 (2013).
- [58] Y.-D. Wang and A. A. Clerk, Reservoir-Engineered Entanglement in Optomechanical Systems, *Phys. Rev. Lett.* **110**, 253601 (2013).
- [59] T. A. Palomaki, J. D. Teufel, R. W. Simmonds, and K. W. Lehnert, Entangling mechanical motion with microwave fields, *Science* **342**, 710 (2013).
- [60] H. Flayac and V. Savona, Heralded Preparation and Readout of Entangled Phonons in a Photonic Crystal Cavity, *Phys. Rev. Lett.* **113**, 143603 (2014).
- [61] J.-Q. Liao, Q.-Q. Wu, and F. Nori, Entangling two macroscopic mechanical mirrors in a two-cavity optomechanical system, *Phys. Rev. A* **89**, 014302 (2014).
- [62] M. Ho, E. Oudot, J.-D. Bancal, and N. Sangouard, Witnessing Optomechanical Entanglement with Photon Counting, *Phys. Rev. Lett.* **121**, 023602 (2018).
- [63] S. Barzanjeh, E. S. Redchenko, M. Peruzzo, M. Wulf, D. P. Lewis, G. Arnold, and J. M. Fink, Stationary entangled radiation from micromechanical motion, *Nature (London)* **570**, 480 (2019).
- [64] Y.-F. Jiao, S.-D. Zhang, Y.-L. Zhang, A. Miranowicz, L.-M. Kuang, and H. Jing, Nonreciprocal Optomechanical Entanglement against Backscattering Losses, *Phys. Rev. Lett.*

- 125**, 143605 (2020).
- [65] D.-G. Lai, J.-Q. Liao, A. Miranowicz, and F. Nori, NoiseTolerant Optomechanical Entanglement via Synthetic Magnetism, *Phys. Rev. Lett.* **129**, 063602 (2022).
- [66] J. Huang, D.-G. Lai, and J.-Q. Liao, Thermal-noise-resistant optomechanical entanglement via general dark-mode control, *Phys. Rev. A* **106**, 063506 (2022).
- [67] R. Riedinger, A. Wallucks, I. Marinković, C. Löschnauer, M. Aspelmeyer, S. Hong, and S. Gröblacher, Remote quantum entanglement between two micromechanical oscillators, *Nature (London)* **556**, 473 (2018).
- [68] C. F. Ockeloen-Korppi, E. Damskægg, J.-M. Pirkkalainen, M. Asjad, A. A. Clerk, F. Massel, M. J. Woolley, and M. A. Sillanpää, Stabilized entanglement of massive mechanical oscillators, *Nature (London)* **556**, 478 (2018).
- [69] S. Kotler, G. A. Peterson, E. Shojaei, F. Lecocq, K. Cicak, A. Kwiatkowski, S. Geller, S. Glancy, E. Knill, R. W. Simmonds, J. Aumentado, and J. D. Teufel, Direct observation of deterministic macroscopic entanglement, *Science* **372**, 622 (2021).
- [70] L. M. de Lépinay, C. F. Ockeloen-Korppi, M. J. Woolley, and M. A. Sillanpää, Quantum mechanics-free subsystem with mechanical oscillators, *Science* **372**, 625 (2021).
- [71] W. Chen, P. Roelli, H. Hu, S. Verlekar, S. P. Amirtharaj, A. I. Barreda, T. J. Kippenberg, M. Kovylyna, E. Verhagen, A. Martínez, and C. Galland, Continuous-wave frequency upconversion with a molecular optomechanical nanocavity, *Science* **374**, 1264 (2021).
- [72] A. Xomalis, X. Zheng, R. Chikkaraddy, Z. Koczor-Benda, E. Miele, E. Rosta, G. A. E. Vandenbosch, A. Martínez, and J. J. Baumberg, Detecting mid-infrared light by molecular frequency upconversion in dual-wavelength nanoantennas, *Science* **374**, 1268 (2021).
- [73] G. S. Agarwal, Vacuum-Field Rabi Splittings in Microwave Absorption by Rydberg Atoms in a Cavity, *Phys. Rev. Lett.* **53**, 1732 (1984).
- [74] F. Zou, L. Du, Y. Li, and H. Dong, Amplifying Frequency Up-Converted Infrared Signals with a Molecular Optomechanical Cavity, *Phys. Rev. Lett.* **132**, 153602 (2024).
- [75] S. Mubeen, S. Zhang, N. Kim, S. Lee, S. Kramer, H. Xu, and M. Moskovits, Plasmonic properties of gold nanoparticles separated from a gold mirror by an ultrathin oxide, *Nano Lett.* **12**, 2088 (2012).
- [76] R. Zhang, Y. Zhang, Z. Dong, S. Jiang, C. Zhang, L. Chen, L. Zhang, Y. Liao, J. Aizpurua, Y. Luo, J. Yang, and J. Hou, Chemical mapping of a single molecule by plasmon-enhanced Raman scattering, *Nature (London)* **498**, 82 (2013).
- [77] See Supplemental Material for detailed derivation of the single-photon optomechanical coupling coefficient and the effective Hamiltonian involving two collective vibrational modes.
- [78] C. P. Sun, Y. Li, and X. F. Liu, Quasi-Spin-Wave Quantum Memories with a Dynamical Symmetry, *Phys. Rev. Lett.* **91**, 147903 (2003).
- [79] C. Emary and T. Brandes, Quantum Chaos Triggered by Precursors of a Quantum Phase Transition: The Dicke Model, *Phys. Rev. Lett.* **90**, 044101 (2003).
- [80] C. W. Gardiner and P. Zoller, *Quantum Noise* (Springer, Berlin, 2000).
- [81] I. S. Gradshteyn and I. M. Ryzhik, *Table of Integrals, Series, and Products* (Academic, New York, 2014).
- [82] G. Vidal and R. F. Werner, Computable measure of entanglement, *Phys. Rev. A* **65**, 032314 (2002).
- [83] M. B. Plenio, Logarithmic Negativity: A Full Entanglement Monotone That is not Convex, *Phys. Rev. Lett.* **95**, 090503 (2005).
- [84] R. Simon, Peres-Horodecki Separability Criterion for Continuous Variable Systems, *Phys. Rev. Lett.* **84**, 2726 (2000).
- [85] H. Huang and G. S. Agarwal, General linear transformations and entangled states, *Phys. Rev. A* **49**, 52 (1994).

Supplementary Material for ‘‘Collective Quantum Entanglement in Molecular Cavity Optomechanics’’

S1. MICROSCOPIC DERIVATION OF THE SINGLE-PHOTON OPTOMECHANICAL COUPLING COEFFICIENT

The interaction Hamiltonian between the molecule including the electronic and vibrational states and the plasmonic cavity mode can be described as ($\hbar = 1$)

$$H = \omega_p a^\dagger a + \omega_v b^\dagger b + \omega_e \sigma_+ \sigma_- + \lambda \omega_v \sigma_+ \sigma_- (b^\dagger + b) - \mu (\sigma_+ + \sigma_-) E, \quad (\text{S1})$$

where a (a^\dagger) and b (b^\dagger) are, respectively, the annihilation (creation) operators of plasmonic cavity mode with resonance frequency ω_p and the vibrational mode with the resonance frequency ω_v . The electronic state of the molecule is described by the raising operator $\sigma_+ = |e\rangle\langle g|$ and lowering operator $\sigma_- = |g\rangle\langle e|$ with the excited state $|e\rangle$ and the ground state $|g\rangle$, and ω_e is the energy separation between the two states. The coupling between the electronic state and the vibrational mode is characterized by the Franck-Condon factor λ . The parameter μ is the induced Raman dipole, which describes the interaction between the electronic state and the quantized electromagnetic field of plasmonic cavity mode $E = \sqrt{\hbar\omega_p/(2\varepsilon_0 V_p)}(a^\dagger + a)$, where V_p is the effective mode volume of plasmonic cavity and ε_0 is the vacuum permittivity.

By applying the polaron transformation defined by the operator $U = \exp[-\lambda\sigma_+\sigma_-(b^\dagger - b)]$, we can obtain the transformed Hamiltonian

$$H_1 = \omega_p a^\dagger a + \omega_v b^\dagger b + \tilde{\omega}_e \sigma_+ \sigma_- - f (a^\dagger + a) [\sigma_+ e^{\lambda(b^\dagger - b)} + \sigma_- e^{-\lambda(b^\dagger - b)}], \quad (\text{S2})$$

where $\tilde{\omega}_e = \omega_e - \lambda^2 \omega_v$ and $f = \mu \sqrt{\hbar\omega_p/(2\varepsilon_0 V_p)}$. In the rotating frame defined by $V(t) = \exp(-iH_0 t)$ with $H_0 = \omega_p a^\dagger a + \omega_v b^\dagger b + \tilde{\omega}_e \sigma_+ \sigma_-$, the Hamiltonian H_1 becomes

$$H_2(t) = -f (a^\dagger e^{i\omega_p t} + a e^{-i\omega_p t}) [\sigma_+ e^{i\tilde{\omega}_e t} e^{\lambda(b^\dagger e^{i\omega_v t} - b e^{-i\omega_v t})} + \sigma_- e^{-i\tilde{\omega}_e t} e^{-\lambda(b^\dagger e^{i\omega_v t} - b e^{-i\omega_v t})}]. \quad (\text{S3})$$

Based on the Hamiltonian $H_2(t)$, we project the second-order perturbation term onto the ground state of the electronic state,

$$\begin{aligned} & \langle g | \sigma_- e^{-i\tilde{\omega}_e t} e^{-\lambda(b^\dagger e^{i\omega_v t} - b e^{-i\omega_v t})} \sigma_+ e^{i\tilde{\omega}_e t'} e^{\lambda(b^\dagger e^{i\omega_v t'} - b e^{-i\omega_v t'})} | g \rangle f^2 (a^\dagger e^{i\omega_p t} + a e^{-i\omega_p t}) (a^\dagger e^{i\omega_p t'} + a e^{-i\omega_p t'}) \\ &= e^{-\lambda(b^\dagger e^{i\omega_v t} - b e^{-i\omega_v t})} e^{\lambda(b^\dagger e^{i\omega_v t'} - b e^{-i\omega_v t'})} e^{-i\tilde{\omega}_e(t-t')} f^2 (a^\dagger e^{i\omega_p t} + a e^{-i\omega_p t}) (a^\dagger e^{i\omega_p t'} + a e^{-i\omega_p t'}) \\ &\approx [1 + \lambda(b^\dagger e^{i\omega_v t'} - b e^{-i\omega_v t'} - b^\dagger e^{i\omega_v t} + b e^{-i\omega_v t})] e^{-i\tilde{\omega}_e(t-t')} f^2 (a^\dagger e^{i\omega_p t} + a e^{-i\omega_p t}) (a^\dagger e^{i\omega_p t'} + a e^{-i\omega_p t'}), \end{aligned} \quad (\text{S4})$$

then the effective Hamiltonian between the plasmonic cavity mode and the vibrational mode can be obtained as

$$\int_{-\infty}^T dt \int_{-\infty}^t dt' \lambda f^2 (b^\dagger e^{i\omega_v t'} - b e^{-i\omega_v t'} - b^\dagger e^{i\omega_v t} + b e^{-i\omega_v t}) e^{-i\tilde{\omega}_e(t-t')} (a^\dagger e^{i\omega_p t} + a e^{-i\omega_p t}) (a^\dagger e^{i\omega_p t'} + a e^{-i\omega_p t'}). \quad (\text{S5})$$

Referring to Eq. (S5), after carrying out a series of calculations, we can derive $b^\dagger a^\dagger a$, $ba^\dagger a$, $b^\dagger aa^\dagger$ and baa^\dagger terms.

On the other hand, the effective coupling between the cavity mode and the vibrational mode can be rewritten as

$$\langle g | \mathcal{T} e^{-i \int_{-\infty}^T H_2(t) dt} | g \rangle \approx 1 - i \int_{-\infty}^T \langle g | H_2(t) | g \rangle dt, \quad (\text{S6})$$

where \mathcal{T} is the time-ordering operator. By comparing the two Eqs. (S5) and (S6), we can obtain the effective Hamiltonian

$$\langle g | H_2(t) | g \rangle = (g_v b^\dagger e^{i\omega_v t} + g_v^* b e^{-i\omega_v t}) a^\dagger a, \quad (\text{S7})$$

where we introduce the single-photon optomechanical coupling coefficient

$$g_v \approx -2\lambda f^2 M^{-1}(v) = -2\lambda f^2 \left[\frac{\omega_v + \tilde{\omega}_e}{(\omega_v + \tilde{\omega}_e)^2 - \omega_p^2} - \frac{\omega_v - \tilde{\omega}_e}{(\omega_v - \tilde{\omega}_e)^2 - \omega_p^2} - \frac{2\tilde{\omega}_e}{\tilde{\omega}_e^2 - \omega_p^2} \right]. \quad (\text{S8})$$

By comparing Eq. (S8) with the expression for $g_v = -(\omega_p/\varepsilon_0 V_p) \sqrt{\hbar/(2m\omega_v)} (\partial\alpha/\partial x)$ derived by phenomenological method, we can obtain the isotropic Raman tensor element

$$\frac{\partial\alpha}{\partial x} = \frac{2\lambda f^2}{M(v)} \frac{\varepsilon_0 V_p}{\omega_p} \sqrt{\frac{2m\omega_v}{\hbar}} = \frac{\lambda|\mu|^2}{M(v)\hbar} \sqrt{\frac{2m\omega_v}{\hbar}}, \quad (\text{S9})$$

where α is the Raman polarizability and x is the molecular displacement.

S2. DERIVATION OF THE EFFECTIVE HAMILTONIAN INVOLVING TWO COLLECTIVE VIBRATIONAL MODES

Here we provide a detailed derivation of the effective Hamiltonian for the two-coupled collective vibrational modes. Specifically, in the regime of large cavity-mode decay, the three-mode molecular optomechanical system, consisting of one cavity mode and two collective vibrational modes, is reduced to a two-coupled collective mode system by adiabatically eliminating the cavity mode. Consequently, the effective Hamiltonian for this two-mode system can be obtained. To this end, we start from the linearized quantum Langevin equations

$$\delta\dot{a}(t) = -(i\Delta + \kappa)\delta a(t) - i \sum_{l=1}^2 G_l [\delta B_l^\dagger(t) + \delta B_l(t)] + \sqrt{2\kappa} a_{\text{in}}(t), \quad (\text{S10a})$$

$$\delta\dot{B}_1(t) = -(i\omega_1 + \gamma_1)\delta B_1(t) - iG_1^* \delta a(t) - iG_1 \delta a^\dagger(t) + \sqrt{2\gamma} B_{1,\text{in}}(t), \quad (\text{S10b})$$

$$\delta\dot{B}_2(t) = -(i\omega_2 + \gamma_2)\delta B_2(t) - iG_2^* \delta a(t) - iG_2 \delta a^\dagger(t) + \sqrt{2\gamma} B_{2,\text{in}}(t), \quad (\text{S10c})$$

where $\omega_{l=1,2} = \omega_v$ is the resonance frequency for the l th collective vibrational mode, other parameters and variables have been defined in the main text. For convenience, below we assume that the linearized collective optomechanical coupling strengths G_1 and G_2 are real. To obtain the two-coupled vibrational mode system, we consider that the system works in the parameter regime $\omega_l \gg \kappa \gg \{\gamma_l, \gamma_l\}$. In this case, the solution for the fluctuation operator $\delta a(t)$ can be obtained as

$$\begin{aligned} \delta a(t) = & \delta a(0) e^{-(\kappa+i\Delta)t} - iG_1 \left(\frac{1 - e^{-(\kappa+i\Delta+i\omega_1)t}}{\kappa + i(\Delta + \omega_1)} \delta B_1^\dagger(t) + \frac{1 - e^{-(\kappa+i\Delta-i\omega_1)t}}{\kappa + i(\Delta - \omega_1)} \delta B_1(t) \right) \\ & - iG_2 \left(\frac{1 - e^{-(\kappa+i\Delta+i\omega_2)t}}{\kappa + i(\Delta + \omega_2)} \delta B_2^\dagger(t) + \frac{1 - e^{-(\kappa+i\Delta-i\omega_2)t}}{\kappa + i(\Delta - \omega_2)} \delta B_2(t) \right) + A_{\text{in}}(t), \end{aligned} \quad (\text{S11})$$

where $\delta a(0)$ is the initial value of $\delta a(t)$, and

$$A_{\text{in}}(t) = \sqrt{2\kappa} e^{-(\kappa+i\Delta)t} \int_0^t a_{\text{in}}(s) e^{(\kappa+i\Delta)s} ds \quad (\text{S12})$$

is the new noise operator associated with cavity mode. Here we consider the time scale $t \gg 1/\kappa$ and ignore the initial value $\delta a(0)$, then the solution for $\delta a(t)$ is approximated as

$$\begin{aligned} \delta a(t) \approx & -\frac{iG_1}{\kappa + i(\Delta + \omega_1)} \delta B_1^\dagger(t) - \frac{iG_1}{\kappa + i(\Delta - \omega_1)} \delta B_1(t) - \frac{iG_2}{\kappa + i(\Delta + \omega_2)} \delta B_2^\dagger(t) \\ & - \frac{iG_2}{\kappa + i(\Delta - \omega_2)} \delta B_2(t) + A_{\text{in}}(t). \end{aligned} \quad (\text{S13})$$

By substituting Eq. (S13) into Eqs. (S10b) and (S10c), the equations of motion become

$$\begin{aligned} \delta\dot{B}_1(t) = & \left(\frac{G_1^2}{\kappa - i(\Delta - \omega_1)} - \frac{G_1^2}{\kappa + i(\Delta + \omega_1)} \right) \delta B_1^\dagger(t) + \left(\frac{G_1^2}{\kappa - i(\Delta + \omega_1)} - \frac{G_1^2}{\kappa + i(\Delta - \omega_1)} - \gamma_1 - i\omega_1 \right) \delta B_1(t) \\ & + \left(\frac{G_1 G_2}{\kappa - i(\Delta - \omega_2)} - \frac{G_1 G_2}{\kappa + i(\Delta + \omega_2)} \right) \delta B_2^\dagger(t) + \left(\frac{G_1 G_2}{\kappa - i(\Delta + \omega_2)} - \frac{G_1 G_2}{\kappa + i(\Delta - \omega_2)} \right) \delta B_2(t) \\ & - iG_1 A_{\text{in}}(t) - iG_1 A_{\text{in}}^\dagger(t) + \sqrt{2\gamma_1} B_{1,\text{in}}(t), \end{aligned} \quad (\text{S14a})$$

$$\begin{aligned} \delta\dot{B}_2(t) = & \left(\frac{G_1 G_2}{\kappa - i(\Delta - \omega_1)} - \frac{G_1 G_2}{\kappa + i(\Delta + \omega_1)} \right) \delta B_1^\dagger(t) + \left(\frac{G_1 G_2}{\kappa - i(\Delta + \omega_1)} - \frac{G_1 G_2}{\kappa + i(\Delta - \omega_1)} \right) \delta B_1(t) \\ & + \left(\frac{G_2^2}{\kappa - i(\Delta - \omega_2)} - \frac{G_2^2}{\kappa + i(\Delta + \omega_2)} \right) \delta B_2^\dagger(t) + \left(\frac{G_2^2}{\kappa - i(\Delta + \omega_2)} - \frac{G_2^2}{\kappa + i(\Delta - \omega_2)} - \gamma_2 - i\omega_2 \right) \delta B_2(t) \\ & - iG_2 A_{\text{in}}(t) - iG_2 A_{\text{in}}^\dagger(t) + \sqrt{2\gamma_2} B_{2,\text{in}}(t). \end{aligned} \quad (\text{S14b})$$

Based on Eqs. (S14), we perform the rotating-wave approximation by discarding the $\delta B_1^\dagger(t)$ term in Eq. (S14a) and $\delta B_2^\dagger(t)$ term in Eq. (S14b), then the equations become

$$\begin{aligned} \delta \dot{B}_1(t) = & \left(\frac{G_1^2}{\kappa - i(\Delta + \omega_1)} - \frac{G_1^2}{\kappa + i(\Delta - \omega_1)} - \gamma_1 - i\omega_1 \right) \delta B_1(t) + \left(\frac{G_1 G_2}{\kappa - i(\Delta - \omega_2)} - \frac{G_1 G_2}{\kappa + i(\Delta + \omega_2)} \right) \delta B_2^\dagger(t) \\ & + \left(\frac{G_1 G_2}{\kappa - i(\Delta + \omega_2)} - \frac{G_1 G_2}{\kappa + i(\Delta - \omega_2)} \right) \delta B_2(t) - iG_1 A_{\text{in}}(t) - iG_1 A_{\text{in}}^\dagger(t) + \sqrt{2\gamma_1} B_{1,\text{in}}(t), \end{aligned} \quad (\text{S15a})$$

$$\begin{aligned} \delta \dot{B}_2(t) = & \left(\frac{G_1 G_2}{\kappa - i(\Delta - \omega_1)} - \frac{G_1 G_2}{\kappa + i(\Delta + \omega_1)} \right) \delta B_1^\dagger(t) + \left(\frac{G_1 G_2}{\kappa - i(\Delta + \omega_1)} - \frac{G_1 G_2}{\kappa + i(\Delta - \omega_1)} \right) \delta B_1(t) \\ & + \left(\frac{G_2^2}{\kappa - i(\Delta + \omega_2)} - \frac{G_2^2}{\kappa + i(\Delta - \omega_2)} - \gamma_2 - i\omega_2 \right) \delta B_2(t) - iG_2 A_{\text{in}}(t) - iG_2 A_{\text{in}}^\dagger(t) + \sqrt{2\gamma_2} B_{2,\text{in}}(t). \end{aligned} \quad (\text{S15b})$$

By introducing the resonance frequency shift $\omega_{l,\text{opt}}$ and the optical induced decay rate $\gamma_{l,\text{opt}}$ for l th ($l = 1, 2$) vibrational mode, with

$$\omega_{l,\text{opt}} = \frac{G_l^2(\Delta + \omega_l)}{\kappa^2 + (\Delta + \omega_l)^2} + \frac{G_l^2(\Delta - \omega_l)}{\kappa^2 + (\Delta - \omega_l)^2}, \quad (\text{S16a})$$

$$\gamma_{l,\text{opt}} = \frac{G_l^2 \kappa}{\kappa^2 + (\Delta - \omega_l)^2} - \frac{G_l^2 \kappa}{\kappa^2 + (\Delta + \omega_l)^2}, \quad (\text{S16b})$$

the Eqs. (S15) can be rewritten as

$$\begin{aligned} \delta \dot{B}_1(t) = & -(\Gamma_1 + i\Omega_1) \delta B_1(t) + \left(\frac{G_1 G_2}{\kappa - i(\Delta - \omega_2)} - \frac{G_1 G_2}{\kappa + i(\Delta + \omega_2)} \right) \delta B_2^\dagger(t) \\ & + \left(\frac{G_1 G_2}{\kappa - i(\Delta + \omega_2)} - \frac{G_1 G_2}{\kappa + i(\Delta - \omega_2)} \right) \delta B_2(t) - iG_1 A_{\text{in}}(t) - iG_1 A_{\text{in}}^\dagger(t) + \sqrt{2\gamma_1} B_{1,\text{in}}(t), \end{aligned} \quad (\text{S17a})$$

$$\begin{aligned} \delta \dot{B}_2(t) = & \left(\frac{G_1 G_2}{\kappa - i(\Delta - \omega_1)} - \frac{G_1 G_2}{\kappa + i(\Delta + \omega_1)} \right) \delta B_1^\dagger(t) + \left(\frac{G_1 G_2}{\kappa - i(\Delta + \omega_1)} - \frac{G_1 G_2}{\kappa + i(\Delta - \omega_1)} \right) \delta B_1(t) \\ & - (\Gamma_2 + i\Omega_2) \delta B_2(t) - iG_2 A_{\text{in}}(t) - iG_2 A_{\text{in}}^\dagger(t) + \sqrt{2\gamma_2} B_{2,\text{in}}(t), \end{aligned} \quad (\text{S17b})$$

where $\Omega_l = \omega_l - \omega_{l,\text{opt}}$ and $\Gamma_l = \gamma_l + \gamma_{l,\text{opt}}$ are, respectively, the effective frequency and decay rate for the collective vibrational mode B_l . For simplicity, we present the effective coupling strengths between the two collective vibrational modes B_1 and B_2

$$\mathcal{G}_1 = \frac{G_1 G_2 [\kappa + i(\Delta - \omega_v)]}{\kappa^2 + (\Delta - \omega_v)^2} - \frac{G_1 G_2 [\kappa - i(\Delta + \omega_v)]}{\kappa^2 + (\Delta + \omega_v)^2}, \quad (\text{S18a})$$

$$\mathcal{G}_2 = \frac{G_1 G_2 [\kappa + i(\Delta + \omega_v)]}{\kappa^2 + (\Delta + \omega_v)^2} - \frac{G_1 G_2 [\kappa - i(\Delta - \omega_v)]}{\kappa^2 + (\Delta - \omega_v)^2}. \quad (\text{S18b})$$

Within the parameter regime $\omega_{1,2} \gg \kappa \gg G_{1,2}$ and in the resonance case $\Delta = \omega_v = \omega_{l=1,2}$, \mathcal{G}_1 and \mathcal{G}_2 can be approximated as

$$\mathcal{G}_1 = -\mathcal{G}_2 = \mathcal{G} \approx i \frac{G_1 G_2}{2\omega_v} - \frac{G_1 G_2}{\kappa}, \quad (\text{S19})$$

then the Eqs. (S17) can be simplified to

$$\delta \dot{B}_1(t) = -(\Gamma_1 + i\Omega_1) \delta B_1(t) + \mathcal{G} \delta B_2(t) - \mathcal{G} \delta B_2^\dagger(t) - iG_1 A_{\text{in}}(t) - iG_1 A_{\text{in}}^\dagger(t) + \sqrt{2\gamma_1} B_{1,\text{in}}(t), \quad (\text{S20a})$$

$$\delta \dot{B}_2(t) = -\mathcal{G} \delta B_1^\dagger(t) + \mathcal{G} \delta B_1(t) - (\Gamma_2 + i\Omega_2) \delta B_2(t) - iG_2 A_{\text{in}}(t) - iG_2 A_{\text{in}}^\dagger(t) + \sqrt{2\gamma_2} B_{2,\text{in}}(t). \quad (\text{S20b})$$

Based on the Eqs. (S20), we can obtain the effective Hamiltonian as

$$H_{\text{eff}} = (\Omega_1 - i\Gamma_1) \delta B_1^\dagger \delta B_1 + (\Omega_2 - i\Gamma_2) \delta B_2^\dagger \delta B_2 - i\mathcal{G} (\delta B_1^\dagger - \delta B_1) (\delta B_2^\dagger - \delta B_2). \quad (\text{S21})$$

It can be seen from Eqs. (S19) and (S21) that the coupling strength \mathcal{G} between the two collective vibrational modes is determined by the product of the coupling strength between the cavity mode and each vibrational mode, i.e., $\mathcal{G} \propto G_1 G_2 = \sqrt{M(N-M)} G_v^2$. We also find that the coupling strength \mathcal{G} is much smaller than G_1 and G_2 , which means that the strength of vibration-vibration entanglement is much weaker than that of cavity-vibration entanglement.